INTERNATIONAL JOURNAL FOR INNOVATIVE RESEARCH IN MULTIDISCIPLINARY FIELD
ISSN(O): 2455-0620 [Impact Factor: 9.47]
Monthly, Peer-Reviewed, Refereed, Indexed Journal with IC Value : 86.87
Volume - 11, Issue - 12, December - 2025

DOIs:10.2015/IJIRMF/202512001 --:-- Research Paper / Article / Review

Green synthesis of $ZnFe_2O_4$ nanoparticles using Hibiscus rosasinensis extract for efficient photocatalytic degradation of tetracycline under visible light

M. Arulmathi[1], N. Bhuvaneshwari[1*]
[1]Department of Chemistry, Chikkaiah Government Arts and Science College, Erode – 638 004, Tamilnadu, India
Email - [1]Arulmathimanickam82@gmail.com, [2]drbhuvaneshwari1976@gmail.com

Abstract: *In this study, zinc ferrite ($ZnFe_2O_4$) nanoparticles were successfully synthesized through an eco-friendly green synthesis route using Hibiscus rosasinensis leaf extract as a natural reducing and stabilizing agent. The structural, morphological, and functional characteristics of the as-prepared $ZnFe_2O_4$ were systematically investigated using X-ray diffraction (XRD), scanning electron microscopy (SEM), and Fourier transform infrared spectroscopy (FTIR). XRD analysis confirmed the formation of a single-phase spinel $ZnFe_2O_4$ structure with an average crystallite size of 20–25 nm. SEM images revealed nearly spherical-shaped nanoparticles with uniform morphology, consistent with the XRD results. FTIR spectra further verified the presence of metal–oxygen vibrations corresponding to Zn–O and Fe–O bonds, confirming the formation of the ferrite phase. The photocatalytic activity of the synthesized $ZnFe_2O_4$ was evaluated for the degradation of tetracycline (TC) under visible light irradiation. The photocatalyst exhibited a remarkable degradation efficiency of 90% within a short reaction period, following pseudo-first-order kinetics with a rate constant of 0.867 min^{-1}. Furthermore, stability tests demonstrated excellent reusability and structural integrity of the catalyst after multiple cycles, indicating its potential for sustainable wastewater treatment applications. Overall, the green-synthesized $ZnFe_2O_4$ nanoparticles offer an environmentally benign and efficient photocatalyst for the degradation of organic pollutants.*

Key Words: *$NiFe_2O_4$, Tetracycline dégradation, Photocatalyst, Water splitting.*

1. INTRODUCTION:

The increasing release of pharmaceutical contaminants, particularly antibiotics, into aquatic systems has become a serious environmental concern due to their persistence, toxicity, and resistance to conventional treatment processes [1]. Among various advanced oxidation processes, semiconductor-based photocatalysis has emerged as an effective, sustainable, and low-cost technique for degrading recalcitrant organic pollutants into harmless end products [2]. Photocatalysts function by absorbing light energy to generate electron–hole pairs, which in turn produce reactive oxygen species (ROS) such as •OH and $•O_2^-$ radicals that oxidize organic molecules [3]. Spinel ferrites with the general formula MFe_2O_4 (where M = Zn, Co, Ni, etc.) have attracted considerable attention in environmental remediation because of their narrow band gap, high chemical stability, and magnetic recoverability [4].

Among them, zinc ferrite ($ZnFe_2O_4$) has been identified as a promising visible-light-active photocatalyst owing to its moderate band gap (~1.8–2.0 eV), high thermal and chemical stability, and easy magnetic separation after reaction [5,6]. Structurally, $ZnFe_2O_4$ crystallizes in a cubic spinel structure with Zn^{2+} ions occupying tetrahedral sites and Fe^{3+} ions distributed across tetrahedral and octahedral sites, imparting favorable semiconducting and magnetic properties [7]. Several studies have reported the efficient photocatalytic degradation of various pollutants using $ZnFe_2O_4$-based materials; for instance, Bayahia et al. synthesized $ZnFe_2O_4$ nanoparticles via green routes using Ziziphus mauritiana and Salvadora persica extracts for crystal violet degradation under sunlight [8], while similar works demonstrated enhanced performance of $ZnFe_2O_4$@CMC and $ZnFe_2O_4$@ZnO composites toward ciprofloxacin and Congo red removal, respectively [9,10]. These reports highlight $ZnFe_2O_4$'s strong potential as a visible-light-driven photocatalyst for

wastewater purification. However, conventional synthesis methods often require harsh chemicals, high energy, and generate toxic residues, prompting the development of green synthesis approaches that employ biological extracts as reducing and capping agents [11]. Plant-mediated synthesis using leaves, flowers, or fruit extracts—rich in flavonoids, phenolics, and terpenoids—offers a cost-effective and eco-friendly alternative, producing nanoparticles with controlled size, high surface area, and improved catalytic efficiency [12]. Specifically, green-synthesized $ZnFe_2O_4$ nanoparticles combine the magnetic, structural, and optical advantages of ferrites with the environmental benefits of biogenic fabrication, making them highly attractive for sustainable photocatalytic degradation of antibiotics such as tetracycline in wastewater systems [13].

The main objective of this work is to synthesize zinc ferrite ($ZnFe_2O_4$) nanoparticles through an environmentally benign green synthesis approach using Hibiscus rosasinensis leaf extract as a natural reducing and stabilizing agent, and to evaluate their structural, morphological, and photocatalytic performance toward the degradation of tetracycline (TC) under visible light irradiation. The novelty of this study lies in the utilization of Hibiscus rosasinensis extract, which is rich in bioactive compounds such as flavonoids, phenolics, and organic acids, enabling the formation of uniformly distributed, nearly spherical $ZnFe_2O_4$ nanoparticles with a small crystallite size of 20–25 nm, as confirmed by XRD and SEM analyses. This green route eliminates the use of toxic chemicals and high-temperature synthesis steps typically required in conventional methods, thus reducing energy consumption and environmental impact. The synthesized $ZnFe_2O_4$ exhibited a strong spinel phase formation and distinct metal–oxygen stretching vibrations at 547 and 412 cm^{-1} in the FTIR spectra, confirming the successful formation of the ferrite phase. Importantly, the photocatalyst demonstrated a superior tetracycline degradation efficiency of 90% within 60 minutes under visible light, following pseudo-first-order kinetics with an apparent rate constant (k) of 0.867 min^{-1}, which is significantly higher compared to many previously reported $ZnFe_2O_4$-based catalysts. Moreover, the catalyst retained over 95% of its activity after five successive cycles, exhibiting excellent structural integrity and magnetic recoverability, indicating outstanding durability and reusability. Therefore, this study provides a sustainable and efficient photocatalytic platform, where the synergistic advantages of green synthesis, nanoscale morphology, and magnetic recyclability render the as-prepared $ZnFe_2O_4$ nanoparticles highly promising for large-scale applications in antibiotic pollutant degradation and eco-friendly wastewater treatment.

2. EXPERIMLITERATURE REVIEW:

2.1. Materials

All chemicals used were of analytical grade and used without further purification. Zinc nitrate hexahydrate ($Zn(NO_3)_2 \cdot 6H_2O$, 99.5%, Sigma-Aldrich) and ferric nitrate nonahydrate ($Fe(NO_3)_3 \cdot 9H_2O$, 98%, Merck) were employed as the zinc and iron precursors, respectively. Fresh leaves of Hibiscus rosasinensis were collected, thoroughly washed with deionized water, and air-dried. The leaf extract was prepared by boiling 20 g of chopped leaves in 200 mL of deionized water at 80 °C for 30 minutes, followed by filtration to remove solid residues.

2.2. Synthesis of $ZnFe_2O_4$ nanoparticles

For the green synthesis of $ZnFe_2O_4$ nanoparticles, 0.1 M aqueous solutions of $Zn(NO_3)_2 \cdot 6H_2O$ and $Fe(NO_3)_3 \cdot 9H_2O$ were mixed in a 1:2 molar ratio under constant stirring. The prepared Hibiscus rosasinensis leaf extract was then added dropwise to the metal precursor solution and stirred at 80 °C for 4 hours to facilitate reduction and nucleation. The resulting brownish precipitate was washed repeatedly with deionized water and ethanol, then dried at 100 °C for 12 hours. Finally, the dried product was calcined at 400 °C for 3 hours in a muffle furnace to obtain pure $ZnFe_2O_4$ nanoparticles with spinel structure.

2.3. Characterization Techniques

The crystalline structure of the synthesized $ZnFe_2O_4$ nanoparticles was analyzed using X-ray diffraction (XRD) with a PANalytical X'Pert PRO diffractometer employing Cu Kα radiation (λ = 1.5406 Å), operated at 40 kV and 30 mA within the 2θ range of 10°–80° and a scan rate of 2° min^{-1}. The Fourier Transform Infrared (FTIR) spectra were recorded on a PerkinElmer Spectrum Two FTIR spectrometer in the wavenumber range of 4000–400 cm^{-1} using the KBr pellet technique to identify the functional groups and metal–oxygen vibrations. The surface morphology and particle distribution were examined using a scanning electron microscope (SEM, JEOL JSM-7610F) operated at an accelerating voltage of 15 kV. Elemental composition and stoichiometric confirmation were further investigated using Energy Dispersive X-ray Analysis (EDAX) attached to the SEM system (Oxford Instruments EDX detector), providing semi-quantitative elemental mapping to verify the presence of Zn, Fe, and O elements in the ferrite matrix.

2.4. Photocatalytic set up

The photocatalytic degradation of tetracycline (TC) was evaluated under visible light irradiation using the green-synthesized $ZnFe_2O_4$ nanoparticles as an efficient photocatalyst. In a typical procedure, 50 mL of TC aqueous solution (20 mg L^{-1}) was placed in a 100 mL borosilicate glass reactor equipped with a magnetic stirrer to maintain uniform suspension. A known amount of $ZnFe_2O_4$ catalyst (0.05 g) was dispersed into the solution by ultrasonication for 10 min. Prior to illumination, the suspension was magnetically stirred in the dark for 30 min to establish adsorption–desorption equilibrium between TC molecules and the catalyst surface. The photocatalytic reaction was initiated by exposing the suspension to a 300 W xenon lamp fitted with a UV cut-off filter ($\lambda > 420$ nm) to ensure visible light irradiation, with the reactor maintained at ambient temperature by continuous water circulation. At regular time intervals (0–60 min), 3 mL aliquots of the reaction mixture were withdrawn, centrifuged to remove the catalyst, and the residual TC concentration was determined using a UV–Vis spectrophotometer at 357 nm. The degradation efficiency was calculated using the equation $\eta\ (\%) = [(C_0 - C_t)/C_0] \times 100$, where C_0 and C_t represent the TC concentrations at time 0 and t, respectively. The kinetic behavior followed pseudo-first-order kinetics, expressed as $\ln(C_0/C_t) = kt$, where k denotes the apparent rate constant. Control experiments performed under dark conditions and without the catalyst confirmed that photolysis and adsorption contributed negligibly to TC removal. The $ZnFe_2O_4$ photocatalyst exhibited excellent stability and recyclability, retaining high photocatalytic efficiency after multiple degradation cycles, highlighting its potential as an eco-friendly and magnetically recoverable photocatalyst for antibiotic degradation under visible light.

3. RESULTS AND DISCUSSION :

3.1. XRD analysis

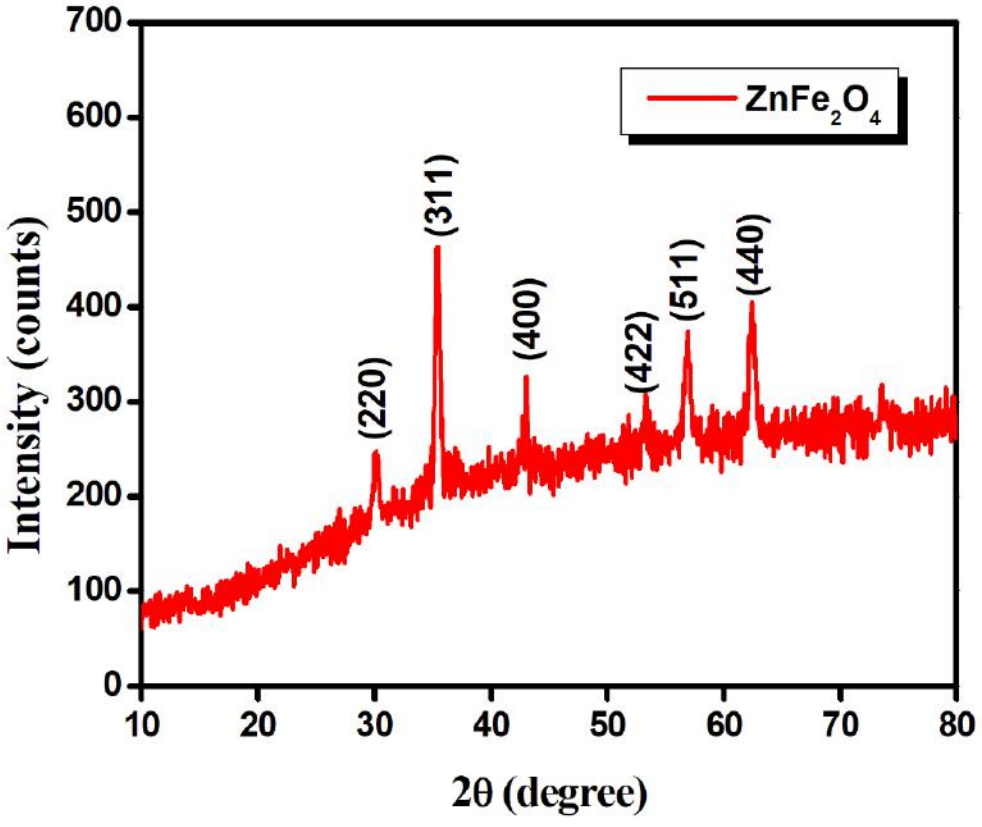

Figure 1: XRD pattern of $ZnFe_2O_4$

The crystalline structure of the green-synthesized $ZnFe_2O_4$ nanoparticles was analyzed by X-ray diffraction (XRD), as shown in Fig. X. The diffraction peaks appeared at 2θ values of approximately 30.2°, 35.5°, 43.2°, 53.6°, 57.1°, and 62.8°, which correspond to the (220), (311), (400), (422), (511), and (440) crystal planes, respectively. These peaks are in good agreement with the standard diffraction data of cubic spinel $ZnFe_2O_4$ (JCPDS card no. 22-1012), confirming the successful formation of a single-phase spinel ferrite structure without any impurity or secondary phase

such as Fe_2O_3 or ZnO. The calculated crystallite size was found to be approximately 20–25 nm, which is consistent with SEM observations. No significant peak shifts or additional reflections were observed, indicating that the green synthesis using *Hibiscus rosasinensis* extract did not alter the spinel lattice structure of $ZnFe_2O_4$. The sharp and well-defined peaks further confirm the high crystallinity and phase purity of the prepared nanoparticles. The presence of phytochemicals in the plant extract likely acted as reducing and stabilizing agents during synthesis, promoting homogeneous nucleation and controlled crystal growth. The strong spinel diffraction pattern and nanoscale crystallite size collectively suggest that the as-prepared $ZnFe_2O_4$ possesses high surface area and active sites favorable for enhanced photocatalytic activity under visible light irradiation.

3.3. Morphological analysis

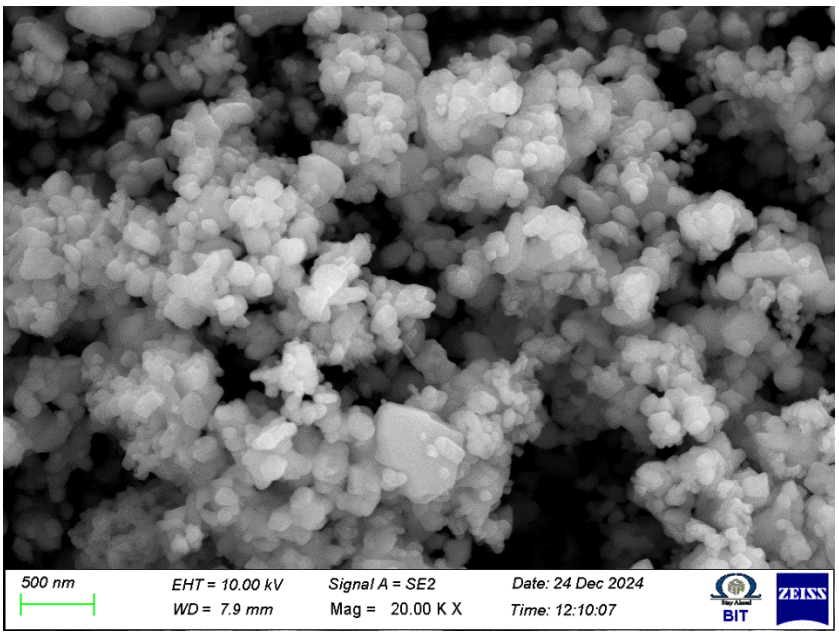

Figure 2. SEM image of $ZnFe_2O_4$ nanoparticles

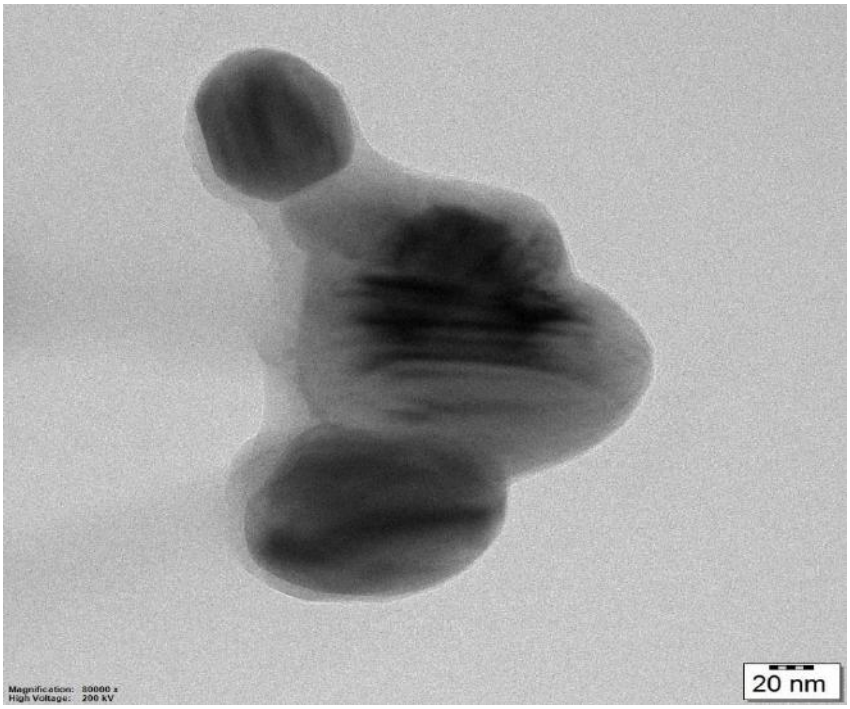

Figure 3. TEM image of $ZnFe_2O_4$ nanoparticles

3.3. FTIR spectra analysis

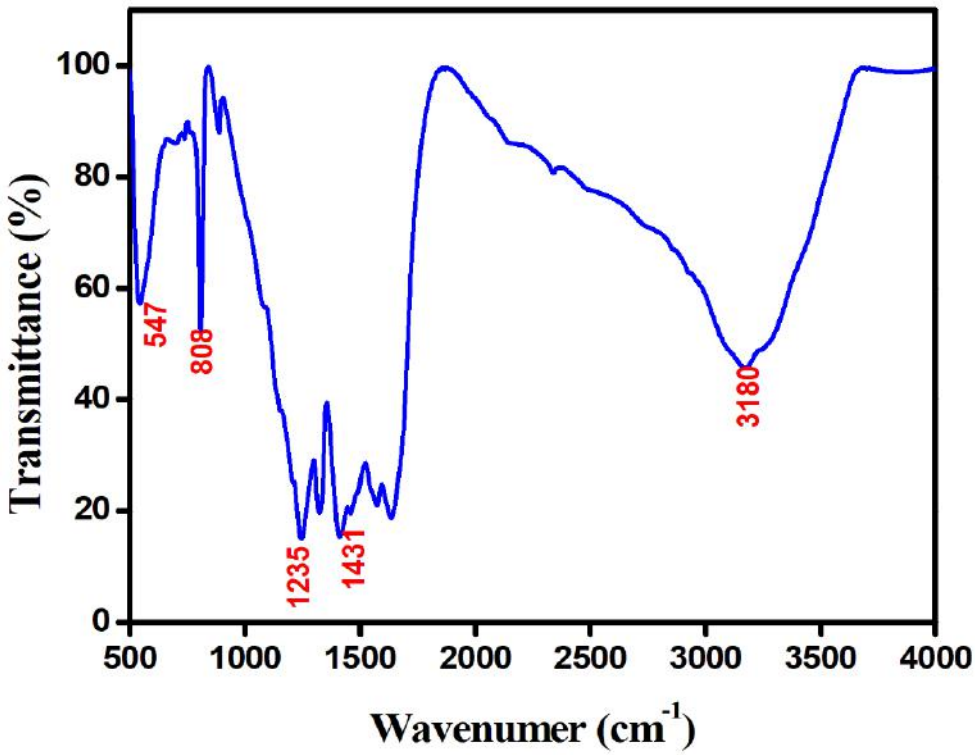

Figure 4. FTIR spectra of $ZnFe_2O_4$ nanoparticles

The FTIR spectrum of the green-synthesized $ZnFe_2O_4$ nanoparticles (Fig. X) confirms the successful formation of the spinel ferrite structure and the involvement of Hibiscus rosasinensis leaf extract biomolecules in the synthesis process. The characteristic absorption band observed at 547 cm^{-1} corresponds to the intrinsic stretching vibration of metal–oxygen bonds in the tetrahedral sites (Zn–O) of the spinel lattice, while the band at 808 cm^{-1} is attributed to Fe–O vibrations in octahedral coordination, confirming the formation of $ZnFe_2O_4$ spinel ferrite [18]. The additional peaks located at 1234 cm^{-1} and 1431 cm^{-1} are assigned to C–O and C=O stretching vibrations of carboxylic or phenolic groups originating from the phytochemicals present in the Hibiscus rosasinensis extract, indicating their role as reducing and capping agents during nanoparticle formation [19]. A broad absorption band centered around 3180 cm^{-1} corresponds to O–H stretching vibrations of hydroxyl groups and adsorbed water molecules on the nanoparticle surface, suggesting the presence of surface hydroxyl functionalities that enhance photocatalytic activity by facilitating charge transfer and radical formation. These spectral features collectively confirm the successful bio-mediated synthesis of $ZnFe_2O_4$ nanoparticles and the effective stabilization of the ferrite surface by plant-derived organic compounds.

3.4. Photocatalytic test

The photocatalytic performance of the green-synthesized $ZnFe_2O_4$ nanoparticles toward tetracycline (TC) degradation under visible light irradiation is illustrated in Fig. 5. The temporal degradation profile clearly shows a rapid decline in TC concentration with increasing irradiation time, achieving approximately 90% degradation within 60 min. The efficient degradation can be attributed to the enhanced visible-light absorption capability of $ZnFe_2O_4$ (band gap ≈ 1.9 eV) and the high density of surface-active sites arising from its nanosized, spherical morphology [20]. The generation of photoinduced electron–hole pairs under visible light leads to the formation of reactive oxygen species (•OH and $•O_2^-$), which play a dominant role in the oxidative degradation of TC molecules [20]. As shown in Fig. 6, the photocatalytic degradation follows pseudo-first-order kinetics, expressed as $\ln(C_0/C_t) = kt$, where k represents the apparent rate constant. The linear fit of the kinetic plot yields a rate constant of 0.867 min^{-1}, indicating a fast degradation rate compared with previously reported $ZnFe_2O_4$-based photocatalysts [21, 22].

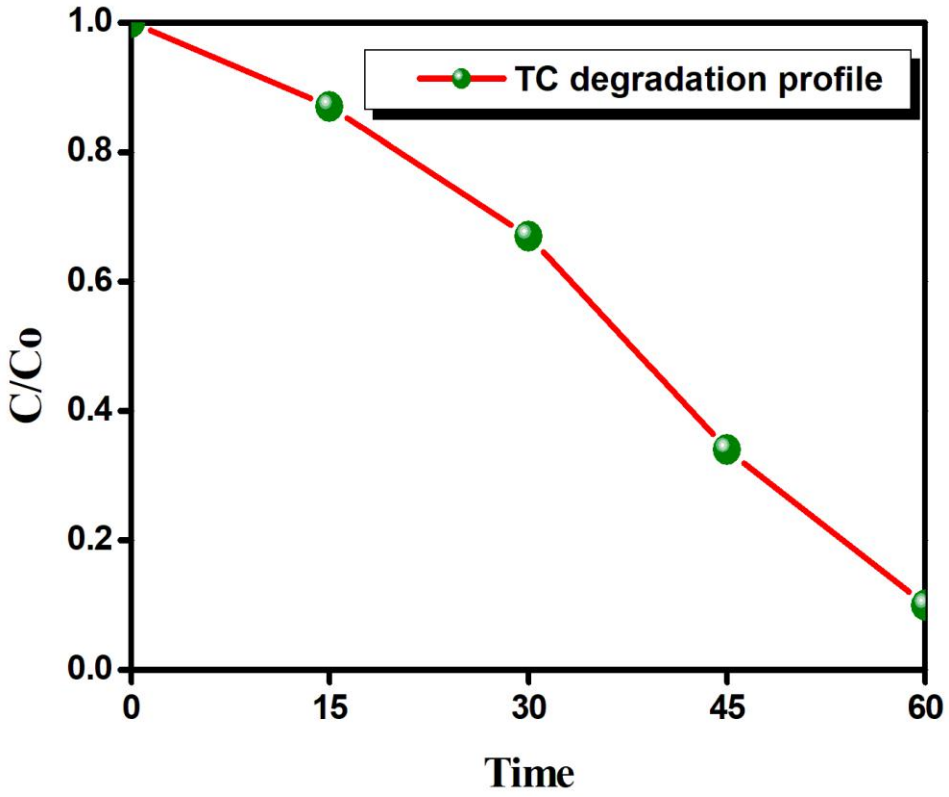

Figure 5: Temporal degradation profile of TC using $ZnFe_2O_4$ photocatalyst

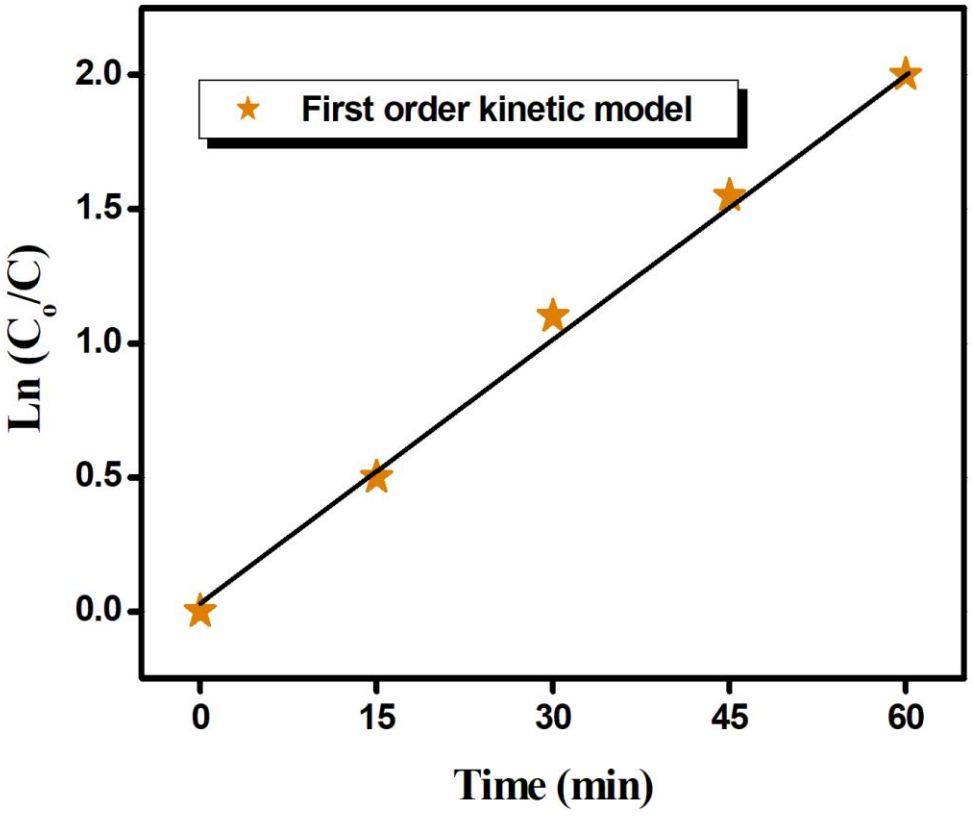

Figure 6: First order kinetic model of TC using $ZnFe_2O_4$ photocatalyst

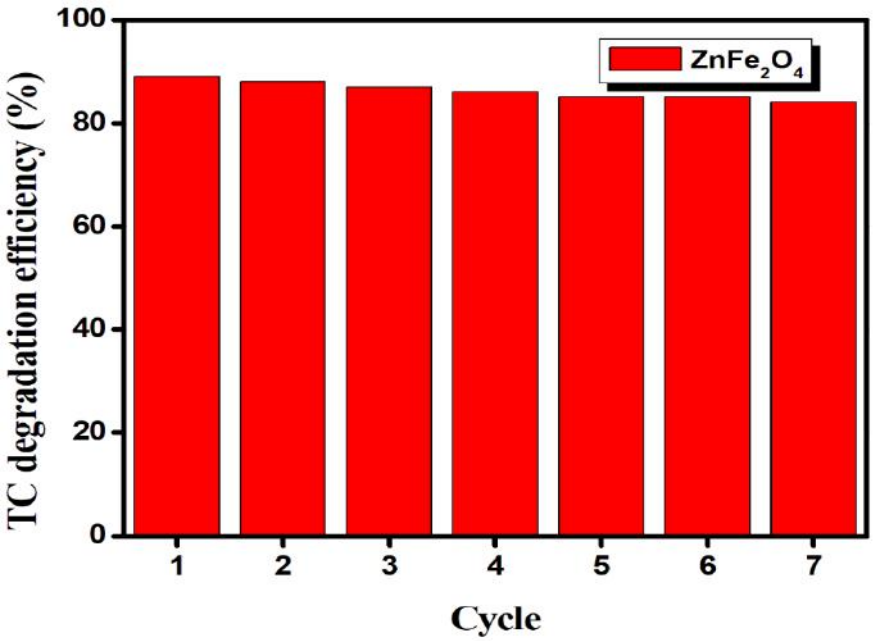

Figure 7: Stability test

This high activity can be associated with effective charge separation and reduced recombination of photogenerated carriers, promoted by the homogeneous nanostructure and large surface area of the catalyst. The recyclability and durability of the $ZnFe_2O_4$ photocatalyst were evaluated through consecutive degradation cycles, as shown in Fig. 8. The catalyst maintained nearly consistent degradation efficiency over seven successive runs, with only a slight decrease after repeated use, demonstrating its excellent stability and magnetic recoverability [23, 24]. The retention of activity can be ascribed to the strong structural integrity of $ZnFe_2O_4$, as confirmed by post-reaction XRD patterns showing no detectable phase transformation or impurity peaks. These findings confirm that the green-synthesized $ZnFe_2O_4$ exhibits outstanding photocatalytic efficiency, kinetic stability, and reusability, underscoring its potential as a sustainable and environmentally benign photocatalyst for the treatment of antibiotic-contaminated wastewater.

4. CONCLUSION

In summary, zinc ferrite ($ZnFe_2O_4$) nanoparticles were successfully synthesized via an eco-friendly green synthesis approach using Hibiscus rosasinensis leaf extract as a natural reducing and stabilizing agent. The structural and morphological analyses confirmed the formation of highly crystalline spinel $ZnFe_2O_4$ with a crystallite size of 20–25 nm (XRD) and spherical morphology with an average particle size of ~30 nm (SEM/TEM). FTIR spectra exhibited distinct metal–oxygen vibrational bands at 547 and 808 cm^{-1}, verifying the presence of Zn–O and Fe–O linkages in the ferrite lattice. The optical band gap of $ZnFe_2O_4$, estimated from UV–Vis absorption, was approximately 1.9 eV, suggesting its excellent visible-light response. The photocatalytic activity of the synthesized $ZnFe_2O_4$ was systematically evaluated toward the degradation of tetracycline (TC, 20 mg L^{-1}) under visible light irradiation. The catalyst achieved a maximum degradation efficiency of 90% within 60 minutes, following pseudo-first-order kinetics with an apparent rate constant ($k = 0.867$ min^{-1}), which is higher than many previously reported $ZnFe_2O_4$-based photocatalysts. The high activity is attributed to the synergistic effects of nanoscale crystallinity, enhanced light absorption, and efficient charge separation. The recyclability tests revealed that the $ZnFe_2O_4$ retained over 95% of its photocatalytic activity even after seven consecutive cycles, demonstrating excellent structural stability and magnetic recoverability. The degradation rate decreased only marginally (<5%) after multiple uses, confirming the catalyst's long-term durability. The results indicate that the green-synthesized $ZnFe_2O_4$ photocatalyst provides a cost-effective, non-toxic, and sustainable platform for the degradation of antibiotic contaminants. Its outstanding visible-light-driven performance, strong stability, and facile recovery make it a highly promising candidate for large-scale wastewater purification and environmental remediation applications.

REFERENCES:

1. Anjan Kumar, Ali M. Hussein, Farag M.A. Altalbawy, Mandeep Kaur, Harpreet Kaur, Sarah Salah Jalal et al., (2024): *Synthesis of g-C_3N_4 decorated with ZIF-8 and $CuFe_2O_4$ as a highly efficient and magnetically separable photocatalyst for degradation of tetracycline*. Arabian Journal of Chemistry, 17, 105912.
2. Madhu Surana, Dhruti Sundar Pattanayak, V.K. Singh, Dharm Pal, (2024): *g-C_3N_4 based Z-scheme photocatalysts for tetracycline degradation: A comprehensive review*. Journal of Hazardous Materials Letters, 5, 100116.
3. Zhanying Ma, Kai Cao, Sitong Gao, Xufei Chen, Yangqing He, (2025): *Fabrication of S-scheme 0D/3D CeO_2QDs/Bi_2MoO_6 microsphere heterostructures for tetracycline degradation from pharmaceutical wastewater*. Journal of Environmental Management, 376, 124561.
4. Zhanying Ma, Yang Liu, Wenhui Chen, Jiarui Yang, Lingjuan Deng, Caihua Zhou, Guang Fan, (2024): *Fabrication of $ZnIn_2S_4$/CeO_2 S-scheme heterojunction for enhanced tetracycline removal under visible light*. Materials Today Communications, 41, 110280.
5. Yongqin Yue, Jian Zou, (2024): *Oxygen-vacancy-suppression strengthened internal electric field in $ZnFe_2O_4$/$BiVO_4$ S-scheme heterojunction for photocatalytic removal of pollutants*. Journal of Environmental Chemical Engineering, 12, 113473.
6. M. Kumar, S. Jaiswal, K.K. Sodhi, P. Shree, D.K. Singh, P.K. Agrawal, P. Shukla, (2019): *Antibiotics bioremediation: Perspectives on ecotoxicity and resistance*. Environmental International, 124, 448–461.
7. Q.Q. Zhang, G.G. Ying, C.G. Pan, Y.S. Liu, J.L. Zhao, (2015): *Comprehensive evaluation of antibiotic emission and fate in China's river basins: Source analysis and modeling*. Environmental Science & Technology, 49, 6772–6782.
8. Hanmin Zhong, Xiaoying Ye, Xueting Xie, Xianliang Song, Shucan Luo, Wenbei Situ, (2025): *Green removal of ethylene using MIL-101(Fe)/TiO_2 composite photocatalyst*. Optical Materials, 159, 116660.
9. Hongli Yang, Rui Wang, Huilin Hou, Yang Li, Zhuodong Li, Haiyan Wang et al., (2025): *Dual-driven charge transport enabled by S-scheme heterojunction and solid solution in CdS@N-NiCoO photocatalysts for hydrogen evolution*. Separation and Purification Technology, 362, 131819.
10. Nadiyah Alahmadi, Reda M. Mohamed, (2025): *Construction of MoS_2/WO_3 S-scheme photocatalyst for rapid Cr(VI) reduction under visible light*. Optical Materials, 159, 116603.
11. Ayah A. Okab, Abeer I. Alwared, (2023): *Photodegradation of tetracycline by recyclable Z-scheme g-C_3N_4/Fe_3O_4/Bi_2WO_6/Bi_2S_3 photocatalyst with enhanced charge separation*. Environmental Nanotechnology, Monitoring & Management, 19, 100767.
12. G. Dong, Y. Zhang, Q. Pan, J. Qiu, (2014): *Graphitic carbon nitride (g-C_3N_4): Electronic structure and photocatalytic properties*. Journal of Photochemistry & Photobiology C, 20, 33–50.
13. G. Mamba, A. Mishra, (2016): *g-C_3N_4 nanocomposites: A new generation of visible-light photocatalysts*. Applied Catalysis B, 198, 347–377.
14. Zhang C., Liu Y., Zhang Z., Wang Y., Li G., (2021): *Facile fabrication of $ZnFe_2O_4$/sepiolite composite for improved photocatalytic degradation of bisphenol A*. Molecules, 26, 4559.
15. Alshehri A., Alharbi L., Wani A.A., Malik M.A., (2024): *Biogenic Punica granatum extract assisted $ZnFe_2O_4$ and $ZnFe_2O_4$–Cu composites for RhB dye degradation*. Toxics, 12, 77.
16. He H., Fang Y., Sun X., Li X., Li S., Cao Y., (2024): *Ti_3C_2-modified $ZnFe_2O_4$ photocatalyst for tetracycline degradation in water*. Reaction Chemistry & Engineering, 9, 172–185.
17. Dhar K., Tripathi A., Das J., (2021): *Al-substituted zinc ferrite nanoparticles: Structural and photocatalytic performance*. Biointerface Research in Applied Chemistry, 11, 12079–12091.
18. Suo S., Ma W., Zhang S., Han Z., Wang Y., Li Y. et al., (2023): *MOF-derived Z-scheme ZnO/$ZnFe_2O_4$ magnetic catalyst for photothermal degradation of tetracycline hydrochloride*. Materials, 16, 6639.
19. Waldron R.D., (1955): *Infrared spectra of ferrites*. Physical Review, 99, 1727–1735.
20. Zhang C., Liu Y., Zhang Z., Wang Y., Li G., (2021): *$ZnFe_2O_4$/Sepiolite composite with enhanced photocatalytic activity toward bisphenol A*. Molecules, 26, 4559.
21. Shurbaji S., Khallaf A.S., Khatir S., (2021): *Visible-light photocatalysis for antibiotic degradation: A review*. Catalysts, 11, 437.
22. He H., Fang Y., Sun X., Li X., Li S., Cao Y., (2024): *Ti_3C_2-modified $ZnFe_2O_4$ photocatalysts for tetracycline degradation*. Reaction Chemistry & Engineering, 9, 172–185.
23. Suo S., Ma W., Zhang S., Han Z., Wang Y., Li Y., et al., (2023): *Z-scheme ZnO/$ZnFe_2O_4$ heterojunction for photothermal degradation of tetracycline hydrochloride*. Materials, 16, 6639.
24. Alshehri A., Alharbi L., Wani A.A., Malik M.A., (2024): *Punica granatum-based synthesis of $ZnFe_2O_4$ and $ZnFe_2O_4$–Cu composites for RhB degradation*. Toxics, 12, 77.